

GreenMachine: Automatic Design of Zero-Cost Proxies for Energy-Efficient NAS

Gabriel Cortês Nuno Lourenço Penousal Machado
CISUC/LASI, DEI, University of Coimbra
{cortes,naml,machado}@dei.uc.pt

Abstract

Artificial Intelligence (AI) has driven innovations and created new opportunities across various sectors. However, leveraging domain-specific knowledge often requires automated tools to design and configure models effectively. In the case of Deep Neural Networks (DNNs), researchers and practitioners usually resort to Neural Architecture Search (NAS) approaches, which are resource- and time-intensive, requiring the training and evaluation of numerous candidate architectures. This raises sustainability concerns, particularly due to the high energy demands involved, creating a paradox: the pursuit of the most effective model can undermine sustainability goals. To mitigate this issue, zero-cost proxies have emerged as a promising alternative. These proxies estimate a model's performance without the need for full training, offering a more efficient approach. This paper addresses the challenges of model evaluation by automatically designing zero-cost proxies to assess DNNs efficiently. Our method begins with a randomly generated set of zero-cost proxies, which are evolved and tested using the NATS-Bench benchmark. We assess the proxies' effectiveness using both randomly sampled and stratified subsets of the search space, ensuring they can differentiate between low- and high-performing networks and enhance generalizability. Results show our method outperforms existing approaches on the stratified sampling strategy, achieving strong correlations with ground truth performance, including a Kendall correlation of 0.89 on CIFAR-10 and 0.77 on CIFAR-100 with NATS-Bench-SSS and a Kendall correlation of 0.78 on CIFAR-10 and 0.71 on CIFAR-100 with NATS-Bench-TSS.

1. Introduction

The impact that AI has had on human lives and society spans various domains, from advances in healthcare diagnosis [4] to optimization of trade routes [36], identification of diseases in plants [3], and cyber in-

trusion detection [8]. This technology allows us to improve most fields of study. However, these advancements have a cost. Several issues affect AI systems: racial and gender bias in automated job and loan applications [20], misclassification in critical scenarios due to data manipulation by bad actors [29], job displacement [16, 34], and massive energy consumption [37]. The latter is quantifiable and has grown exponentially in recent years. For instance, the popular GPT-3 model, similar to the models behind OpenAI's ChatGPT, used 1287 MWh in 15 days just for its training [28]. The current "arms race" to develop Large Language Models (LLMs) models with more capabilities will likely increase the number of parameters, thereby ensuring that more recent models will consume even more energy. Moreover, serving millions of users on a daily basis requires a tremendous quantity of processing devices, such as GPUs and/or TPUs, which use a massive amount of energy. The total energy consumption of NVIDIA GPUs, the leading manufacturer of these devices, is expected to surpass the total energy needs of countries such as Belgium or Switzerland [9, 40]. Furthermore, technological companies like Google and Microsoft, which have previously committed to offsetting their carbon emissions, have struggled to maintain these promises due to allocating more resources to AI data centers [17, 30]. This growth is expected to continue, with hardly any restrictions, due to the positive impact this technology has on the population and the economy [15].

Several techniques have been proposed to address the energy consumption problem of AI, particularly of Machine Learning (ML). Reducing the floating-point precision of a model's weights has been shown to enhance energy efficiency, albeit at the tradeoff of some performance [31]. Spiking Neural Networks (SNNs) show promising results due to their sparsity and event-based operation, though they require further hardware-side developments to fulfill their theoretical energy efficiency potential [18, 26]. Using NAS

or Neuroevolution (NE) to search for energy-efficient DNN models has also significantly increased energy efficiency [7]. This approach, however, requires substantial resources since each DNN must undergo a full training process and subsequent evaluation, which may ultimately undermine its potential for minimal energy usage.

In this paper, we present an approach to mitigate the energy consumption problem of NAS. Zero-cost proxies estimate a DNN’s performance without training, with some recent proxies having achieved high correlations with the ground truth, reporting a Kendall correlation of 0.706 on the NATS-Bench-TSS search space with the CIFAR-10 dataset [10], or even 0.741 on the same problem when using an ensemble of four zero-cost proxies [21]. This means that the score given by the zero-cost proxy to a DNN aligns well with its actual performance in terms of accuracy.

Our main contribution is the proposal of an algorithm that automatically generates and optimizes zero-cost proxies using evolution¹. Specifically, we begin with a randomly generated set of proxies that are then modified or evolved over several generations to gradually improve their estimation of model performance. These proxies are evaluated on the NATS-Bench benchmark across the CIFAR-10, CIFAR-100, and ImageNet16-120 datasets. We assess their performance in two ways: 1) on a subset that is a randomly selected sample of the overall search space; and 2) on a stratified subset with a diverse distribution of networks to evaluate the proxies not only on “good” networks but also on those with lower performance. This approach is intended to ensure that the proxies can differentiate between low- and high-performing DNNs, minimizing overfitting and enhancing generalizability.

Experimental results indicate that this approach produced better-performing solutions than similar methods in the literature. We achieved higher correlations on nearly all datasets using a stratification technique to sample networks. Specifically, we obtained a Kendall correlation of 0.89 on CIFAR-10 and 0.77 on CIFAR-100 with NATS-Bench-SSS and a Kendall correlation of 0.78 on CIFAR-10 and 0.71 on CIFAR-100 with NATS-Bench-TSS.

This paper is structured as follows. Section 2 presents the necessary background on Evolutionary Algorithms (EAs), focusing on Genetic Programming (GP), and on zero-cost proxies as well as related work. Section 3 showcases the functioning of the developed algorithm and details the experimental setup. Afterward, Section 4 present the obtained results and a

discussion about them. At last, Section 5 concludes this paper and outlines potential directions for future work.

2. Background and Related Work

2.1. Genetic Programming

GP is an AI technique that allows for the automatic design of programs, expressions, or models with variable length, using the principles of natural selection and evolution (Fig. 1) [13, 38]. When using GP, one needs to specify the set of variables or constants and the set of functions. One of the most commonly used representations of solutions is syntax trees.

The initial set of solutions, called population, is usually created randomly. Some trees are generated with the maximum depth, others have branches with varying depths, and a mix of both approaches is also used.

Individuals are evaluated based on a fitness function that measures their performance on a given problem. The fittest individuals are then probabilistically selected to produce new solutions, or offspring, for the next generation, allowing successful traits to be passed along. Offspring undergo mutation to introduce genetic diversity, helping the population explore a broader range of potential solutions.

In the context of GP, mutation is performed by replacing a sub-tree rooted at a randomly selected node with a newly generated sub-tree, introducing novel structures. Recombination occurs by swapping sub-trees rooted at randomly selected nodes between two individuals, enabling the exchange of genetic material and potentially beneficial traits.

Grammatical Evolution

Grammatical Evolution (GE) is a grammar-based GP that uses a variable-length integer representation [32]. It relies on the production rules of a Context-free Grammar (CFG) to generate solutions. A CFG is defined by a tuple (N, T, P, S) with N being the set of non-terminals, T the set of terminals, P the set of production rules, and $S \in N$ is a start symbol.

The solution generation process from an integer sequence is carried out as follows: the sequence is read from left to right, beginning with S , and a production rule is iteratively applied to expand the leftmost non-terminal symbol. The current item’s value in the sequence determines the production rule to use by calculating its modulo with respect to the number of available expansions for the leftmost non-terminal symbol.

¹The code is publicly available on [Github](#)

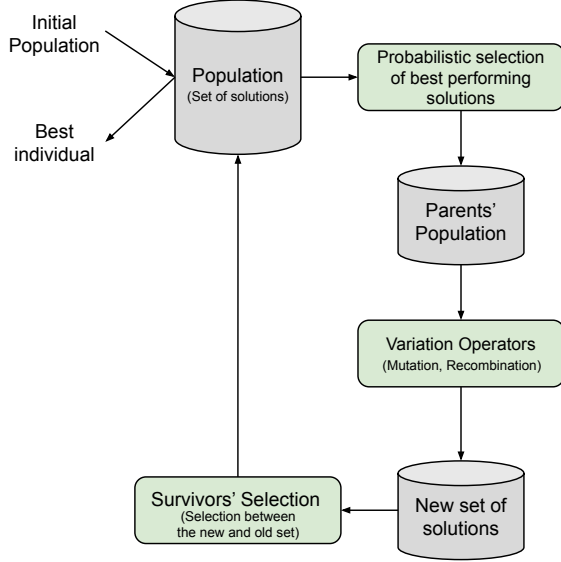


Figure 1. Simplified visualization of the flow of an EA.

Consider the grammar in Fig. 2 with $N = \{\langle \text{expr} \rangle, \langle \text{op} \rangle, \langle \text{trig} \rangle, \langle \text{var} \rangle\}$, $T = \{+, -, \sin, \cos, x, y, (\,)\}$ and $S = \langle \text{expr} \rangle$. Considering a genotype with integer values ranging from 0 to 63, the mapping process is as follows (Fig. 3). First, we begin with the start symbol, $\langle \text{expr} \rangle$, and read the first element of the integer vector. Since there are three options on how to expand the start symbol, we have $46 \bmod 3 = 1$; thus, the start symbol is replaced by its second expansion rule, $\langle \text{trig} \rangle(\langle \text{expr} \rangle)$. Following this, the second value in the genotype is read, and we expand the leftmost non-terminal symbol, repeating the process. This is executed until there are no more non-terminal symbols. It is possible to use a wrapping mechanism instead of terminating the mapping process if there are no more integers to read from the genotype, thus reusing the genotype values.

```

<expr> ::= <expr> <op> <expr>
        | <trig>(<expr>)
        | <var>
<op>   ::= + | -
<trig> ::= sin | cos
<var>  ::= x | y

```

Figure 2. Example of a grammar.

Despite GE’s flexibility and ease of use, it has suffered from issues, such as low locality and high redundancy [24]. To address these limitations, Structured Grammatical Evolution (SGE) [25] was introduced. SGE mitigates these issues by associating each gene

Genotype: [46, 15, 17, 28, 50, 42, 22, 19, 51, 35]

```

<expr>
<trig>(<expr>)  46 mod 3 = 1
cos(<expr>)     15 mod 2 = 1
cos(<var>)      17 mod 3 = 2
cos(x)         28 mod 2 = 0

```

Figure 3. Example of Grammatical Evolution mapping.

with a specific non-terminal and using variable-length integer lists to represent expansion choices. This structure ensures that changing one gene does not affect the derivation choices for other non-terminals, which reduces phenotypic changes and thereby improves locality. Furthermore, the values in each list are constrained by the number of expansion options available for the corresponding non-terminal, eliminating the need for modulo operations and reducing redundancy. Empirical results demonstrate that SGE outperforms GE across various optimization problems.

2.2. Zero-cost proxies

Zero-Shot, also known as the training-free method, is a technique that allows the prediction of the quality of a model without training it [39]. This is achieved through proxies, which are algorithms or mathematical formulas that estimate how good a model might be. These proxies allow us to assess the performance of a DNN model without training it, thus saving resources. Zero-cost proxies are a relatively recent research thread in the ML community since they were introduced in 2018 by Camero et al. [5] and have since been continuously improved. Traditional NAS methods typically require hundreds or thousands of GPU hours and, as such, can significantly benefit from using training-free methods. Zero-cost proxies allow us to predict the performance of a DNN model without training it, and they usually require only a small amount of GPU time or even CPU time to do so. Despite numerous statistical analyses of training-free NAS algorithms, a theoretical analysis of training-free algorithms remains lacking. A comprehensive theoretical examination of this score function is essential to further research in this field [39].

To avoid training many networks to evaluate the correlation between the proxy and the actual accuracy, well-established NAS datasets are used [39]. Among other metrics, these datasets contain the architectures of many networks and their corresponding accuracies.

A pioneer in the field, NASWOT is an algorithm that generates scores reflecting a model’s test accu-

racy without requiring training. It computes these scores based on the network’s activation patterns in response to a single mini-batch [27]. Synflow is a pruning algorithm that aims to prevent the layer collapse problem when pruning a neural network. It was extended as a data-independent estimator of a network’s performance without training it [35]. Inspired by pruning-at-initialization, GradNorm is a proxy metric that computes the sum of the Euclidean norms of the gradients after passing a single mini-batch of training data [1]. TE-NAS is a framework that evaluates network architectures by examining the spectrum of the neural tangent kernel and the number of linear regions in the input space [6]. Zen-NAS is a zero-shot method that measures the expressivity of a DNN by computing its Zen-Score, which is derived from a few forward inferences on randomly initialized networks with random Gaussian inputs [23]. ZiCo demonstrates that high-performance DNNs tend to possess high absolute mean values and low standard deviation values for the gradient and uses that information to estimate the performance of a network [22].

EZNAS proposes a GP approach to automate the discovery of zero-cost proxies for NAS scoring [2] by using the DEAP framework [14]. Each individual’s fitness is determined by the minimum Kendall τ coefficient it achieves across both search spaces. After the evolutionary process, the fittest individual is evaluated on 4000 random networks from the same two search spaces. While EZNAS’s results are competitive with the current state of the art, the authors do not provide details on how the other zero-cost proxies were evaluated, making direct comparisons potentially unfair. Furthermore, EZNAS uses statistics from only a portion of the overall layers of the models and employs a relatively low recombination rate of 40%, which may not be sufficient to generate optimal individuals consistently.

3. Methodology

3.1. Benchmarks

Benchmarking NAS algorithms is challenging due to variations in data preprocessing, evaluation pipelines, and even random seeds. Moreover, fully training a large number of networks requires extensive computational resources, thus making reproducibility difficult for most researchers. To address this issue, some datasets were proposed to standardize the benchmarking process, providing a common ground for comparisons and reducing the required computational resources by delivering the results that would

otherwise require the complete training of many DNN models.

These benchmarks typically include not only the network configuration and its accuracy metric after training but also other data such as latency, number of parameters, and more, enabling a quicker assessment of the proposed NAS method.

NAS-Bench-201 features full graph cells, allowing for a more comprehensive search space, though limited to four nodes and five associated operation options to maintain manageability [11]. Each architecture is trained and evaluated on the CIFAR-10, CIFAR-100, and ImageNet-16-120 image classification datasets. It contains 15,625 architectures. NATS-Bench is a unified benchmark for searching for architecture topology and size [12]. It includes 15,625 candidates for the architecture topology (TSS) and 32,768 for architecture size (SSS). It also presents results for CIFAR-10, CIFAR-100, and ImageNet-16-120. Although not explicitly mentioned in the paper, the authors note in the project’s Github repository² that the topology search space is equivalent to NAS-Bench-201.

3.2. Experimental Setup

The experiments were conducted on a machine running Ubuntu 22.04.3 LTS with two Intel Xeon Silver 4310 CPUs with a clock frequency of 2.10GHz and 12 cores each, 256 GB of RAM, and three NVIDIA RTX A6000 GPUs with 48 GB of GDDR6 RAM. The environment in which they were executed used CUDA 12.1, Python 3.10, and PyTorch 2.3.1.

3.2.1 Networks Sampling

After analyzing the search spaces (Fig. 4), we observed a skew towards networks with high accuracy across both search spaces, regardless of the dataset. Consequently, random sampling does not ensure adequate search space coverage, as it may produce a sample set that is too constrained or biased toward high-performance networks. This bias can result in proxies that fail to distinguish effectively between low- and high-performing networks. To address this issue, we stratified the search space based on test accuracy, creating five groups or bins of networks according to their performance. This approach ensures a diverse set of samples for evaluation. Additionally, we sample 20 networks from each dataset for each search space using this stratification method to maintain a balanced representation across different performance bins.

²<https://github.com/D-X-Y/NATS-Bench>

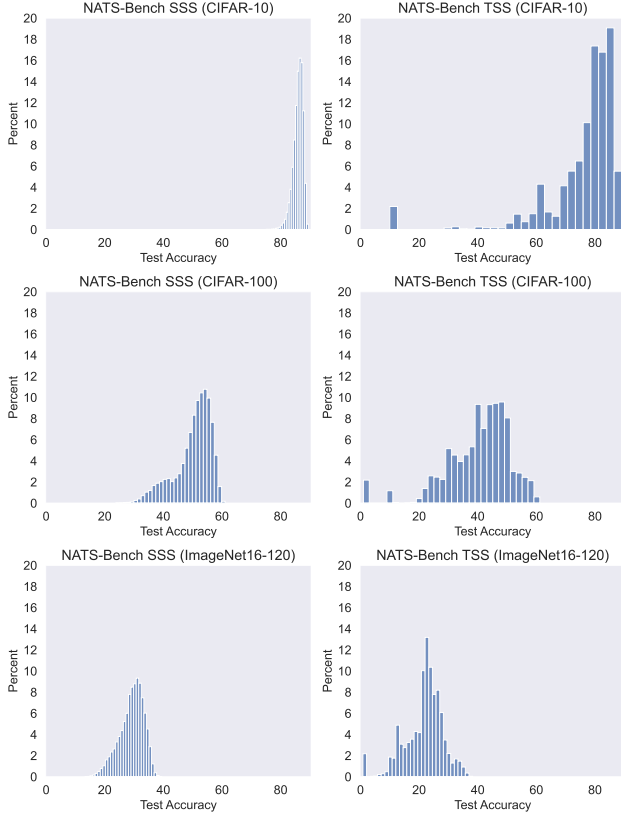


Figure 4. Histograms of test accuracy for the NATS-Bench benchmark across the topology and size search spaces and the CIFAR-10, CIFAR-100, and ImageNet16-120 datasets.

3.2.2 Zero-Cost Proxies Evaluation

We assess the usefulness of the zero-cost proxies using search spaces that comprise architectures of DNNs and their respective test accuracy after training. Specifically, we use the NATS-Bench benchmark [12]. The evaluation uses the zero-cost proxy to score every network sampled. Then we calculate Kendall’s correlation (τ) between the set of scores (S) and the actual test accuracy (A). The τ measures the ordinal association between the two sets according to the following:

Let $S = \{s_1, s_2, \dots, s_n\}$ represent the scores from a zero-cost proxy, and $A = \{a_1, a_2, \dots, a_n\}$ represent the test accuracies.

The Kendall tau correlation coefficient between S and A is given by:

$$\tau = \frac{P - Q}{\sqrt{(P + Q + T)(P + Q + U)}}$$

where:

- P is the number of concordant pairs, i.e., pairs

- (s_i, a_i) and (s_j, a_j) such that $(s_i - s_j)(a_i - a_j) > 0$,
- Q is the number of discordant pairs, i.e., pairs (s_i, a_i) and (s_j, a_j) such that $(s_i - s_j)(a_i - a_j) < 0$,
- T is the number of ties in S , i.e., pairs (s_i, s_j) such that $s_i = s_j$,
- U is the number of ties in A , i.e., pairs (a_i, a_j) such that $a_i = a_j$.

This metric indicates the zero-cost proxy’s suitability for predicting model performance, reflecting the likelihood that a proxy score correlates with the actual model accuracy.

The evaluation function is defined as the sum of the absolute values of the Kendall rank correlation coefficients across all search space and dataset combinations. We use absolute values rather than signed ones to detect any correlation, not solely a positive one.

3.2.3 Feature Extraction

We extract 20 features from each layer of a network. When applicable, these are the weights and gradients of the layer and the weights before and after a forward pass or a backward pass takes place. At first, we consider the randomly initialized network and archive each layer’s weights and gradients. After this, we repeat the complete extraction process in three modes: one where we pass a batch of random data on the network, another where we pass a batch from the dataset, and, last, a mode where we pass a batch from the dataset but perturbed with noise.

Having this archive of network statistics, we then iterate over each of the network’s layers and compute the current individual’s formula. The final score attributed to the network is the mean value of the score of all layers.

3.2.4 Operations

The available operations range from essential mathematical functions like addition, subtraction, element-wise product, and matrix multiplication to specialized computations such as Frobenius norm and eigenvalue ratios. We also include activation functions like ReLU and sigmoid and normalization techniques. Additionally, we provide methods for noise addition, cosine similarity, and logical comparisons. The complete list of operations is presented as supplementary material.

To handle feature extraction from every layer, we ensure that matrices of any dimension are compatible for operations. We do this by flattening the matrices, comparing their lengths, and padding the shorter one with a constant (1). This gives both matrices the same number of elements, allowing them to be reshaped

Table 1. Experimental parameters.

Evolutionary Parameter	Value
Number of runs	5
Number of generations	100
Population size	100
Elitism size	10
Tournament size	5
Crossover rate	90%
Mutation rate	50%
Tree depth	[5, 12]
Num. of evaluated networks	120

back to the original dimensions of the larger matrix. Additionally, we replace invalid tensors with a default tensor of 1 and substitute invalid values within tensors to maintain valid operations and prevent runtime errors, ensuring that no individuals are excluded due to shape mismatches.

3.2.5 Search Algorithm

To perform the search for zero-cost proxies, we used the grammar-based GP approach described in [25], with the parameters detailed in Tab. 1. Specifically, we performed five runs, each for 100 generations, with a population size of 100 individuals. To preserve the best solutions, an elitism size of 10 was applied. Selection was based on tournament selection with a tournament size of 5. The genetic operators were configured with a crossover rate of 90% and a mutation rate of 50%. The evolutionary trees had depths ranging from 5 to 12, and each experiment evaluated 120 networks.

Table 1 lists the used experimental parameters.

4. Results and Discussion

Figure 5 shows the evolution of zero-cost proxies’ performance, measured by the Kendall correlation coefficient (τ), over 100 iterations across NATS-Bench’s two search spaces on the CIFAR-10, CIFAR-100, and ImageNet16-120 datasets, averaged over five runs. In the figure, dashed lines represent performance on the Topology Search Space (TSS), while solid lines indicate performance on the Size Search Space (SSS). The thick solid line illustrates the fitness of the individuals, defined as the sum of the absolute values of the τ scores across the datasets.

Examining the results in Fig. 5, we observe that zero-cost performance on the CIFAR-10 and ImageNet16-120 datasets in the TSS (dashed lines) is lower than in the SSS (solid lines). For CIFAR-100,

the difference is minimal. This suggests that identifying zero-cost proxies in the TSS is more challenging than in the SSS. This difficulty can be attributed to the typical correlation between network size and performance [19]. A proxy that leverages the number of network parameters to estimate performance has a better chance of accurately predicting performance in the SSS. In contrast, extracting performance-related features based on network topology is inherently more complex, which is required to estimate the performance on the TSS.

Additionally, as shown in Fig. 4, the distribution of network performance differs between the search spaces. In the TSS, network performance ranges widely from about 10% (close to random choice) to nearly 95%, while in the SSS, performance is concentrated within narrower accuracy ranges.

Finally, slight decreases in the solid and dashed lines can be observed, particularly in the correlations measured in the SSS search space. Since the quality of the proxies is defined as the sum of the τ correlations across both search spaces, this behavior is expected, as tradeoffs are made to improve correlation in the other search space.

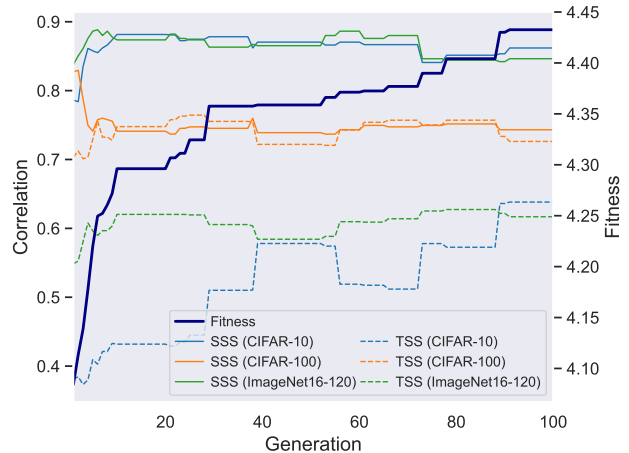


Figure 5. Evolution of the Kendall correlation coefficient on NATS-Bench’s two search spaces and the fitness metric over 100 generations, averaged over 5 runs.

Validating the Zero-Cost Proxies To assess the generalization ability of the zero-cost proxies, we evaluate them on networks that differ from those used in training. Specifically, we test the proxies on 4,500 new networks. We evaluate 30 sets of 150 networks from each search space and dataset, using stratified and non-stratified sampling strategies. This approach ensures that our evaluation covers a diverse range of

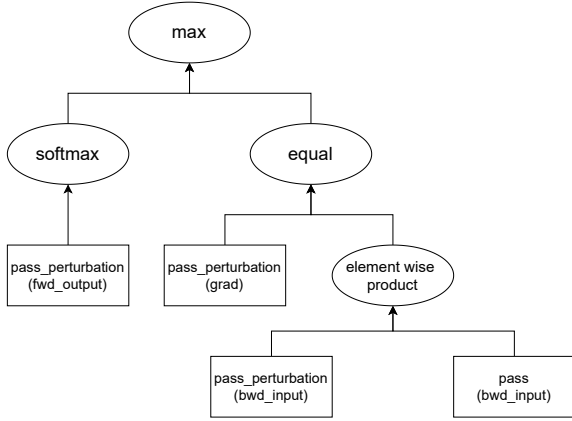


Figure 6. Representation of the GreenMachine-2 solution, where ellipses represent functions and rectangles denote terminal symbols (variables).

architectures, allowing us better to assess the generalization and robustness of the proxies. With 30 sets of networks, we report the mean and standard deviation across these sets.

We implemented state-of-the-art zero-cost proxies from the literature and applied them to the same set of networks to ensure a fair comparison. Additionally, we included a random proxy that generates a random score between 0 and 1 for comparison purposes. Figure 6 depicts the GreenMachine-2 solution, and the formulas for the remaining best solutions discovered by our approach are provided as supplementary material.

Tables 3 and 4 present the validation results for the two sampling strategies using the τ correlation coefficient. The corresponding results for Spearman’s rank correlation are available as supplementary material.

In Tab. 3, where networks are randomly sampled without considering performance representativity, we observe no significant differences among the zero-cost proxies. However, one zero-cost proxy discovered by our approach, GreenMachine-3 (GM-3), outperforms the others on CIFAR-100 when applied to the SSS.

This result can be explained by the fact that the randomly sampled set of networks shows very similar performances, as indicated in Tab. 2. As mentioned previously, if network sampling is not done carefully, the resulting set can consist of models with very similar performance. Observing the standard deviation of the non-stratified set of networks, we see that it is low, indicating high similarity in performance. This reduces the need for proxies to make clear distinctions. However, when evaluating CIFAR-100 on the

SSS, the standard deviation increases, requiring proxies to distinguish between high- and low-performing networks more effectively.

Table 2. Characterization of the networks used for validation of zero-cost proxies. Each cell presents the average accuracy (%) and standard deviation of 30 sets of 150 networks for the non-stratified and stratified versions of the SSS and TSS search spaces across the three different datasets.

	CIFAR-10	CIFAR-100	ImageNet16-120
	Non-Stratified		
SSS	85.98 \pm 1.74	50.13 \pm 6.28	29.19 \pm 4.09
TSS	75.83 \pm 13.76	40.60 \pm 11.06	21.74 \pm 6.36
	Stratified		
SSS	80.71 \pm 4.90	42.95 \pm 9.71	26.47 \pm 6.59
TSS	49.28 \pm 25.15	31.15 \pm 17.21	19.04 \pm 10.96

Concerning the validation where we used a stratified sampling strategy, the zero-cost proxies discovered by our approach can clearly distinguish between low-performing and high-performing networks (see Tab. 3). Our proxies achieve the highest τ correlation across the entire SSS search space, and, on the TSS search space, our solutions surpass those in the literature in all cases except for the ImageNet16-120 dataset. This exception can be explained by the distribution of network performances: as shown in Tab. 2, the TSS ImageNet16-120 stratified version has a low standard deviation, indicating that network performances are very similar in this sample set, and proxies are not required to distinguish between low and high performers.

5. Conclusion

This paper introduces GreenMachine, an algorithm that automatically designs zero-cost proxies using an evolutionary approach. We evaluate the effectiveness of the discovered proxies using the NATS-Bench benchmark across CIFAR-10, CIFAR-100, and ImageNet16-120 datasets.

The solutions discovered by our proposed approach perform better than existing zero-cost proxy methods when distinguishing between low- and high-performing networks. To assess this, we apply stratified sampling to the search space, dividing it into groups based on test accuracy to ensure a representative set of samples for evaluating the proxies. We use the Kendall correlation coefficient to measure the correlation between the proxy scores and network accuracy.

Table 3. Comparison of Zero-Cost proxies on the NATS-Bench benchmark across the CIFAR-10, CIFAR-100, and ImageNet16-120 datasets on the **non-stratified subset**. The presented values are the **mean absolute Kendall correlation coefficient** over 30 runs, multiplied by 100. Bold denotes the best value.

Proxy	SSS (CF-10)	SSS (CF-100)	SSS (IN16-120)	TSS (CF-10)	TSS (CF-100)	TSS (IN16-120)
Random	4.0 ± 2.2	4.4 ± 3.9	4.5 ± 3.6	4.4 ± 3.4	4.2 ± 2.8	4.1 ± 3.1
#Params	67.4 ± 3.3	53.5 ± 4.5	65.6 ± 3.3	37.3 ± 4.6	35.1 ± 5.5	28.3 ± 5.1
Synflow [35]	76.8 ± 1.9	59.0 ± 4.1	79.5 ± 2.3	37.4 ± 5.7	35.1 ± 5.7	35.6 ± 4.6
Gradnorm [1]	18.7 ± 5.0	48.4 ± 4.8	36.8 ± 5.8	14.7 ± 5.9	5.9 ± 4.4	6.7 ± 3.8
NASWOT [27]	38.1 ± 4.2	16.1 ± 5.3	40.7 ± 4.2	43.0 ± 4.6	38.0 ± 4.3	38.5 ± 5.8
TE-NAS [6]	34.2 ± 4.0	28.1 ± 5.8	38.8 ± 5.3	24.8 ± 4.8	13.0 ± 5.7	8.2 ± 6.0
Zen-NAS [23]	72.6 ± 2.5	47.0 ± 5.0	67.0 ± 2.9	12.6 ± 5.1	17.0 ± 5.8	21.9 ± 4.8
ZiCo [22]	73.1 ± 2.1	56.3 ± 3.1	73.5 ± 2.8	39.0 ± 5.5	35.6 ± 5.3	36.0 ± 4.8
EZNAS [2]	72.5 ± 2.5	48.7 ± 4.1	57.0 ± 2.9	61.1 ± 3.5	60.9 ± 3.8	54.7 ± 4.6
GM-1 (Ours)	51.8 ± 3.2	55.9 ± 4.3	49.7 ± 3.8	50.2 ± 4.8	48.1 ± 4.5	39.1 ± 4.8
GM-2 (Ours)	68.5 ± 2.9	62.4 ± 3.9	78.0 ± 1.7	33.7 ± 5.2	31.0 ± 4.9	31.5 ± 4.7
GM-3 (Ours)	75.6 ± 2.5	66.8 ± 3.3	70.2 ± 2.7	8.9 ± 4.9	6.7 ± 4.4	28.8 ± 5.0

Table 4. Comparison of Zero-Cost proxies on the NATS-Bench benchmark across the CIFAR-10, CIFAR-100, and ImageNet16-120 datasets on the **stratified subset**. The presented values are the **mean absolute Kendall correlation coefficient** over 30 runs, multiplied by 100. Bold denotes the best value.

Proxy	SSS (CF-10)	SSS (CF-100)	SSS (IN16-120)	TSS (CF-10)	TSS (CF-100)	TSS (IN16-120)
Random	5.1 ± 3.4	4.5 ± 2.9	4.2 ± 3.7	4.3 ± 3.3	3.4 ± 2.9	4.0 ± 3.0
#Params	75.8 ± 2.4	48.9 ± 4.5	59.4 ± 3.5	38.1 ± 3.7	42.9 ± 4.8	31.3 ± 4.1
Synflow [35]	80.6 ± 1.8	59.8 ± 3.9	71.3 ± 2.8	73.9 ± 2.1	45.9 ± 3.1	39.9 ± 4.7
Gradnorm [1]	41.0 ± 3.9	59.1 ± 2.2	47.4 ± 3.6	59.5 ± 2.4	20.9 ± 5.0	7.1 ± 4.9
NASWOT [27]	53.3 ± 3.5	14.9 ± 7.1	34.7 ± 5.1	71.2 ± 2.5	52.7 ± 3.2	43.2 ± 4.0
TE-NAS [6]	53.8 ± 2.8	28.6 ± 6.2	36.3 ± 4.6	14.5 ± 5.3	21.0 ± 7.2	11.6 ± 5.1
Zen-NAS [23]	77.2 ± 1.9	47.2 ± 4.7	59.0 ± 3.7	31.0 ± 4.9	18.2 ± 5.7	22.0 ± 5.7
ZiCo [22]	79.5 ± 1.9	58.1 ± 3.7	80.9 ± 1.2	75.0 ± 2.2	48.3 ± 3.5	62.1 ± 2.6
EZNAS [2]	82.8 ± 0.9	64.4 ± 2.6	70.7 ± 2.1	57.4 ± 2.3	70.0 ± 2.2	66.2 ± 3.4
GM-1 (Ours)	61.9 ± 2.6	65.3 ± 2.9	67.6 ± 2.1	78.3 ± 2.0	70.5 ± 2.2	64.3 ± 3.0
GM-2 (Ours)	82.7 ± 1.4	76.9 ± 1.6	85.6 ± 0.9	65.5 ± 2.9	55.8 ± 3.2	55.8 ± 3.5
GM-3 (Ours)	88.8 ± 0.9	74.4 ± 1.3	79.4 ± 1.3	39.1 ± 4.5	29.6 ± 4.6	57.0 ± 3.4

The results show that we achieve better performance on nearly all datasets, demonstrating the ability to effectively differentiate between low- and high-performing DNNs while minimizing overfitting and enhancing generalizability. Notably, on the CIFAR-10 dataset using the NATS-Bench-SSS benchmark, GreenMachine achieved a Kendall correlation of 0.89,

and on the NATS-Bench-TSS benchmark with the same dataset, a Kendall correlation of 0.78.

5.1. Future Work

In this work, we evolved and tested the generated solutions on only two benchmarks. Using other search spaces and datasets could enhance the generalizabil-

ity of our results, allowing for a better assessment of the proxy’s effectiveness across multiple problem domains.

Allied with evaluating the individuals on more search spaces, it might be relevant to experiment using more specialized selection operators, such as lexica selection [33], to promote solutions that perform well across a diverse range of tasks.

One potential enhancement to the evolutionary algorithm involves using ephemeral constants, which could fine-tune the relative importance of features within the solutions, improving the quality of the proxies.

References

- [1] Mohamed S. Abdelfattah, Abhinav Mehrotra, Lukasz Dudziak, and Nicholas Donald Lane. Zero-cost proxies for lightweight NAS. In *9th International Conference on Learning Representations, ICLR 2021, Virtual Event, Austria, May 3-7, 2021*. OpenReview.net, 2021. 4, 8, 13
- [2] Yash Akhauri, Juan Pablo Muñoz, Nilesh Jain, and Ravi Iyer. EZNAS: evolving zero-cost proxies for neural architecture scoring. In *Advances in Neural Information Processing Systems 35: Annual Conference on Neural Information Processing Systems 2022, NeurIPS 2022, New Orleans, LA, USA, November 28 - December 9, 2022*, 2022. 4, 8, 13
- [3] Anwar Abdullah Alatawi, Shahd Maadi Alomani, Najd Ibrahim Alhawiti, and Muhammad Ayaz. Plant disease detection using ai based vgg-16 model. *International Journal of Advanced Computer Science and Applications*, 2022. 1
- [4] S. A. Alowais, S. S. Alghamdi, N. Alsuhebany, T. Alqahtani, A. I. Alshaya, S. N. Almohareb, A. Aldaireem, M. Alrashed, K. Bin Saleh, H. A. Badreldin, M. S. Al Yami, S. Al Harbi, and A. M. Albekairy. Revolutionizing healthcare: the role of artificial intelligence in clinical practice. *BMC Medical Education*, 23(1):689, 2023. 1
- [5] Andrés Camero, Jamal Toutouh, and Enrique Alba. Low-cost recurrent neural network expected performance evaluation. *CoRR*, abs/1805.07159, 2018. 3
- [6] Wuyang Chen, Xinyu Gong, and Zhangyang Wang. Neural architecture search on imagenet in four GPU hours: A theoretically inspired perspective. In *9th International Conference on Learning Representations, ICLR 2021, Virtual Event, Austria, May 3-7, 2021*. OpenReview.net, 2021. 4, 8, 13
- [7] Gabriel Cortês, Nuno Lourenço, and Penousal Machado. Towards physical plausibility in neuroevolution systems. In *Applications of Evolutionary Computation - 27th European Conference, EvoApplications 2024, Held as Part of EvoStar 2024, Aberystwyth, UK, April 3-5, 2024, Proceedings, Part II*, pages 76–90. Springer, 2024. 2
- [8] Bibhu Dash, Md Meraj Ansari, Pawankumar Sharma, and Azad Ali. Threats and opportunities with ai-based cyber security intrusion detection: A review. *International Journal of Software Engineering & Applications*, 2022. 1
- [9] Alex de Vries. The growing energy footprint of artificial intelligence. *Joule*, 7(10):2191–2194, 2023. 1
- [10] Peijie Dong, Lujun Li, Xinglin Pan, Zimian Wei, Xiang Liu, Qiang Wang, and Xiaowen Chu. Parzc: Parametric zero-cost proxies for efficient NAS. *CoRR*, abs/2402.02105, 2024. 2
- [11] Xuanyi Dong and Yi Yang. NAS-Bench-201: Extending the scope of reproducible neural architecture search. In *8th International Conference on Learning Representations, ICLR 2020, Addis Ababa, Ethiopia, April 26-30, 2020*. OpenReview.net, 2020. 4
- [12] Xuanyi Dong, Lu Liu, Katarzyna Musial, and Bogdan Gabrys. NATS-Bench: Benchmarking NAS algorithms for architecture topology and size. *IEEE Trans. Pattern Anal. Mach. Intell.*, 44(7):3634–3646, 2022. 4, 5
- [13] A. E. Eiben and James E. Smith. *Introduction to Evolutionary Computing, Second Edition*. Springer, 2015. 2
- [14] Félix-Antoine Fortin, François-Michel De Rainville, Marc-André Gardner, Marc Parizeau, and Christian Gagné. DEAP: evolutionary algorithms made easy. *J. Mach. Learn. Res.*, 13:2171–2175, 2012. 4
- [15] Jason Furman and Robert Seamans. Ai and the economy. Working Paper 24689, National Bureau of Economic Research, 2018. 1
- [16] Orlando Gomes. I, robot: the three laws of robotics and the ethics of the peopleless economy. *AI Ethics*, 4(2):257–272, 2024. 1
- [17] Google. 2024 Environmental Report. <https://sustainability.google/reports/google-2024-environmental-report/>, 2024. [Accessed 05-10-2024]. 1
- [18] Muhammad Hamis Haider, Hao Zhang, S. Deivalaskhmi, G. Lakshmi Narayanan, and Seok-Bum Ko. *Is Neuromorphic Computing the Key to Power-Efficient Neural Networks: A Survey*, pages 91–113. Springer Nature Switzerland, Cham, 2024. 1
- [19] Joel Hestness, Sharan Narang, Newsha Ardalani, Gregory F. Diamos, Heewoo Jun, Hassan Kianinejad, Md. Mostofa Ali Patwary, Yang Yang, and Yanqi Zhou. Deep learning scaling is predictable, empirically. *CoRR*, abs/1712.00409, 2017. 6
- [20] Adheesh Kadiresan, Yuvraj Baweja, and Obi Ogbanufe. *Bias in AI-Based Decision-Making*, pages 275–285. Springer International Publishing, Cham, 2022. 1
- [21] Junghyup Lee and Bumsu Ham. AZ-NAS: assembling zero-cost proxies for network architecture search. In *IEEE/CVF Conference on Computer Vision and Pattern Recognition, CVPR 2024, Seattle, WA, USA, June 16-22, 2024*, pages 5893–5903. IEEE, 2024. 2
- [22] Guihong Li, Yuedong Yang, Kartikeya Bhardwaj, and Radu Marculescu. Zico: Zero-shot NAS via inverse coefficient of variation on gradients. In *The Eleventh International Conference on Learning Representations, ICLR 2023, Kigali, Rwanda, May 1-5, 2023*. OpenReview.net, 2023. 4, 8, 13

- [23] Ming Lin, Pichao Wang, Zhenhong Sun, Heseng Chen, Xiuyu Sun, Qi Qian, Hao Li, and Rong Jin. Zen-nas: A zero-shot NAS for high-performance image recognition. In *2021 IEEE/CVF International Conference on Computer Vision, ICCV 2021, Montreal, QC, Canada, October 10-17, 2021*, pages 337–346. IEEE, 2021. 4, 8, 13
- [24] Nuno Lourenço, Francisco B. Pereira, and Ernesto Costa. SGE: A structured representation for grammatical evolution. In *Artificial Evolution - 12th International Conference, Evolution Artificielle, EA 2015, Lyon, France, October 26-28, 2015. Revised Selected Papers*, pages 136–148. Springer, 2015. 3
- [25] Nuno Lourenço, Filipe Assunção, Francisco B. Pereira, Ernesto Costa, and Penousal Machado. Structured grammatical evolution: A dynamic approach. In *Handbook of Grammatical Evolution*, pages 137–161. Springer, 2018. 3, 6
- [26] Wolfgang Maass. Networks of spiking neurons: The third generation of neural network models. *Neural Networks*, 10(9):1659–1671, 1997. 1
- [27] Joe Mellor, Jack Turner, Amos Storkey, and Elliot J Crowley. Neural architecture search without training. In *Proceedings of the 38th International Conference on Machine Learning*, pages 7588–7598. PMLR, 2021. 4, 8, 13
- [28] David A. Patterson, Joseph Gonzalez, Urs Hölzle, Quoc V. Le, Chen Liang, Lluís-Miquel Munguia, Daniel Rothchild, David R. So, Maud Texier, and Jeff Dean. The carbon footprint of machine learning training will plateau, then shrink. *Computer*, 55(7):18–28, 2022. 1
- [29] Miguel A. Ramirez, Song-Kyoo Kim, Hussam M. N. Al Hamadi, Ernesto Damiani, Young-Ji Byon, Tae-Yeon Kim, Chung-Suk Cho, and Chan Yeob Yeun. Poisoning attacks and defenses on artificial intelligence: A survey. *CoRR*, abs/2202.10276, 2022. 1
- [30] Dan Robinson. Microsoft’s carbon emissions up nearly 30 <https://www.msn.com/en-us/money/other/microsofts-carbon-emissions-up-nearly-30-thanks-to-ai/ar-BB1mvgao>, 2024. [Accessed 05-10-2024]. 1
- [31] Babak Rokh, Ali Azarpeyvand, and Alireza Khanteymoori. A comprehensive survey on model quantization for deep neural networks in image classification. *ACM Trans. Intell. Syst. Technol.*, 14(6), 2023. 1
- [32] Conor Ryan, JJ Collins, and Michael O. Neill. Grammatical evolution: Evolving programs for an arbitrary language. In *Genetic Programming*, pages 83–96, Berlin, Heidelberg, 1998. Springer Berlin Heidelberg. 2
- [33] Lee Spector. Assessment of problem modality by differential performance of lexibase selection in genetic programming: a preliminary report. In *Genetic and Evolutionary Computation Conference, GECCO '12, Philadelphia, PA, USA, July 7-11, 2012, Companion Material Proceedings*, pages 401–408. ACM, 2012. 9
- [34] Grace Su. Unemployment in the AI age. *AI Matters*, 3(4):35–43, 2018. 1
- [35] Hidenori Tanaka, Daniel Kunin, Daniel L. K. Yamins, and Surya Ganguli. Pruning neural networks without any data by iteratively conserving synaptic flow. In *Advances in Neural Information Processing Systems 33: Annual Conference on Neural Information Processing Systems 2020, NeurIPS 2020, December 6-12, 2020, virtual*, 2020. 4, 8, 13
- [36] Rama Vaddy. AI and ML for Transportation Route Optimization. *International Transactions in Machine Learning*, 5(5):1–19, 2023. 1
- [37] Aimee van Wynsberghe. Sustainable AI: AI for sustainability and the sustainability of AI. *AI Ethics*, 1(3): 213–218, 2021. 1
- [38] M.-J. Willis, H.G. Hiden, P. Marenbach, B. McKay, and G.A. Montague. Genetic programming: an introduction and survey of applications. In *Second International Conference On Genetic Algorithms In Engineering Systems: Innovations And Applications*, pages 314–319, 1997. 2
- [39] Meng-Ting Wu and Chun-Wei Tsai. Training-free neural architecture search: A review. *ICT Express*, 10(1): 213–231, 2024. 3
- [40] Mengwei Xu, Wangsong Yin, Dongqi Cai, Rongjie Yi, Daliang Xu, Qipeng Wang, Bingyang Wu, Yihao Zhao, Chen Yang, Shihe Wang, Qiyang Zhang, Zhenyan Lu, Li Zhang, Shangguang Wang, Yuan Chun Li, Yunxin Liu, Xin Jin, and Xuanzhe Liu. A survey of resource-efficient LLM and multimodal foundation models. *CoRR*, abs/2401.08092, 2024. 1

Supplementary Material

Table 5. List of unary operations used in GreenMachine.

Operation	Description
Abs	Compute the absolute value element-wise.
Add noise	Add random noise (standard normal distribution) to a tensor.
Determinant	Calculate the determinant of a matrix.
Element-wise invert	Invert elements of a tensor element-wise.
Exp	Apply the exponential function element-wise.
Frobenius norm	Compute the Frobenius norm of a tensor.
Gaussian initialization	Initialize a tensor with the random values from the standard normal distribution.
Greater than zero	Check if elements are greater than zero.
Heaviside	Compute the Heaviside step function for each element.
L1 norm	Compute the L1 norm of a tensor.
Less than zero	Check if elements are less than zero.
Log	Apply the natural logarithm element-wise.
Log determinant	Compute the log determinant of a matrix.
Normalized sum	Return the sum of tensor elements normalized.
Normalization	Scale tensor values to a 0-1 range.
Num elements	Return the number of elements in a tensor.
Ones like	Create a tensor of ones with the same shape as the input.
ReLU	Apply the ReLU activation element-wise.
Sigmoid	Apply the sigmoid function element-wise.
Sign	Extract the sign of each element.
Softmax	Apply the softmax function element-wise.
Squared power	Raise each element to the power of 2.
Transpose	Compute the transpose of a matrix.
Zeros like	Create a tensor of zeros with the same shape as the input.

Table 6. List of binary operations used in GreenMachine.

Operation	Description
Cosine similarity	Calculates cosine similarity between tensors.
Element-wise product	Multiplies tensors element-wise.
Equal	Checks element-wise equality of tensors.
Greater than	Checks element-wise if one tensor is greater than another.
Kullback–Leibler divergence	Computes the Kullback-Leibler divergence.
Less than	Checks element-wise if one tensor is less than another.
Matrix multiplication	Performs matrix multiplication.
Max	Returns the element-wise maximum of two tensors.
Min	Returns the element-wise minimum of two tensors.
Subtraction	Subtracts one tensor from another element-wise.
Sum	Adds two tensors element-wise.

GreenMachine-1: `(greater_than((mat_mul(pass_noise_wt, (greater_than((kl_div(pass_noise_grad, pass_noise_wt), subtract(pass_noise_fwd_output, pass_perturbation_bwd_input))))), random_wt))`

GreenMachine-2: `max(softmax(pass_perturbation_fwd_output), equal(pass_perturbation_grad, element_wise_product(pass_perturbation_bwd_input, pass_bwd_input)))`

GreenMachine-3: `cosine_similarity(softmax(cosine_similarity(pass_perturbation_bwd_output, pass_fwd_output)), (greater_than(greater_than(pass_noise_fwd_output, cosine_similarity(pass_perturbation_grad, less_than(less_than(equal((equal(abs((max(transpose(pass_noise_bwd_output), normalize(less_than_zero(pass_fwd_output))))), (greater_than(gaussian_init((kl_div(power(pass_noise_bwd_input), normalized_sum(pass_grad))), element_wise_product(kl_div(cosine_similarity(pass_perturbation_fwd_output, random_grad), (sum(random_wt, pass_perturbation_grad))), greater_than(pass_bwd_output, (max(pass_perturbation_fwd_output, pass_bwd_input))))))))), (subtract(element_wise_invert(pass_perturbation_wt), gaussian_init(determinant(pass_perturbation_bwd_input))))), (greater_than(kl_div((min(random_grad, pass_noise_bwd_input)), pass_noise_fwd_output), (mat_mul((element_wise_product(pass_noise_fwd_input, pass_perturbation_fwd_output)), ones_like(sum((mat_mul(frobenius_norm(pass_fwd_input), frobenius_norm(pass_perturbation_bwd_output)), numel(l1_norm(pass_noise_grad))))))))), greater_than(pass_noise_fwd_input, (subtract(sum(random_wt, heaviside(pass_noise_bwd_output)), softmax((mat_mul(sum(greater_than(pass_fwd_output, cosine_similarity(pass_perturbation_bwd_output, pass_perturbation_fwd_input)), (sum((min(pass_bwd_output, pass_noise_wt)), cosine_similarity(pass_grad, pass_noise_grad))))), sigmoid(frobenius_norm(normalize(pass_fwd_output))))))))), random_wt))`

Figure 7. Formulas of the best solutions found.

Table 7. Comparison of Zero-Cost proxies on the NATS-Bench benchmark across the CIFAR-10, CIFAR-100, and ImageNet16-120 datasets on the **non-stratified subset**. The presented values are the **mean absolute Spearman correlation coefficient** over 30 runs, multiplied by 100. Bold denotes the best value.

Proxy	SSS (CF-10)	SSS (CF-100)	SSS (IN16-120)	TSS (CF-10)	TSS (CF-100)	TSS (IN16-120)
Random	5.9 ± 3.3	6.6 ± 5.7	6.8 ± 5.4	6.4 ± 5.1	6.2 ± 4.3	6.1 ± 4.7
#Params	85.6 ± 2.8	71.5 ± 5.4	82.9 ± 3.4	51.9 ± 5.9	48.9 ± 7.3	39.3 ± 6.7
Synflow [35]	92.6 ± 1.3	78.2 ± 4.1	93.2 ± 1.6	52.8 ± 7.4	50.1 ± 7.6	50.0 ± 6.3
Gradnorm [1]	27.6 ± 7.5	67.0 ± 5.9	52.4 ± 7.5	21.1 ± 8.4	8.7 ± 6.2	9.5 ± 5.4
NASWOT [27]	54.0 ± 5.3	23.5 ± 7.6	56.6 ± 5.5	60.0 ± 5.7	54.0 ± 5.6	54.2 ± 7.4
TE-NAS [6]	48.9 ± 5.5	40.1 ± 8.0	54.3 ± 7.3	32.8 ± 7.1	16.6 ± 8.1	11.6 ± 8.0
Zen-NAS [23]	89.7 ± 1.8	64.9 ± 6.1	84.2 ± 2.8	17.8 ± 7.6	24.4 ± 8.1	31.1 ± 6.9
ZiCo [22]	90.2 ± 1.7	75.7 ± 3.3	89.9 ± 2.1	54.9 ± 6.9	51.2 ± 7.0	51.1 ± 6.3
EZNAS [2]	89.6 ± 1.9	67.0 ± 4.9	76.0 ± 3.0	79.6 ± 3.3	78.7 ± 3.8	72.4 ± 4.8
GM-1 (Ours)	70.4 ± 3.5	72.2 ± 4.9	68.6 ± 4.4	67.6 ± 5.6	65.1 ± 5.4	54.4 ± 5.9
GM-2 (Ours)	86.2 ± 2.6	80.4 ± 3.7	93.1 ± 1.0	47.3 ± 7.0	44.4 ± 7.0	44.8 ± 6.3
GM-3 (Ours)	91.2 ± 1.9	84.2 ± 3.2	87.7 ± 2.3	13.7 ± 7.0	10.6 ± 6.2	40.4 ± 6.9

Table 8. Comparison of Zero-Cost proxies on the NATS-Bench benchmark across the CIFAR-10, CIFAR-100, and ImageNet16-120 datasets on the **stratified subset**. The presented values are the **mean absolute Spearman correlation coefficient** over 30 runs, multiplied by 100. Bold denotes the best value.

Proxy	SSS (CF-10)	SSS (CF-100)	SSS (IN16-120)	TSS (CF-10)	TSS (CF-100)	TSS (IN16-120)
Random	7.5 ± 5.0	6.6 ± 4.4	6.2 ± 5.3	6.4 ± 4.8	5.0 ± 4.3	6.0 ± 4.4
#Params	91.6 ± 1.7	66.4 ± 5.4	76.9 ± 3.8	51.1 ± 4.9	58.4 ± 6.0	43.6 ± 5.5
Synflow [35]	94.3 ± 1.1	78.4 ± 4.0	87.0 ± 2.3	91.1 ± 1.2	65.2 ± 3.8	55.8 ± 5.7
Gradnorm [1]	59.5 ± 5.0	80.9 ± 1.7	67.1 ± 4.4	79.0 ± 2.4	30.3 ± 6.9	10.5 ± 7.4
NASWOT [27]	73.0 ± 3.9	21.9 ± 10.3	48.8 ± 6.8	88.7 ± 2.0	72.1 ± 3.6	60.0 ± 4.8
TE-NAS [6]	74.3 ± 3.2	40.9 ± 8.6	51.0 ± 6.4	31.3 ± 6.6	26.5 ± 10.1	15.8 ± 7.3
Zen-NAS [23]	92.5 ± 1.2	64.7 ± 5.6	76.4 ± 3.8	48.5 ± 6.8	27.0 ± 8.9	32.2 ± 8.0
ZiCo [22]	93.9 ± 1.1	76.8 ± 3.8	94.9 ± 0.5	91.0 ± 1.4	67.3 ± 4.1	80.4 ± 2.7
EZNAS [2]	95.9 ± 0.4	82.9 ± 2.3	88.8 ± 1.6	76.1 ± 2.4	88.5 ± 1.5	84.7 ± 3.1
GM-1 (Ours)	81.6 ± 2.5	84.7 ± 2.3	86.8 ± 1.6	92.8 ± 1.7	87.3 ± 2.0	82.7 ± 2.8
GM-2 (Ours)	95.8 ± 0.7	92.4 ± 0.9	97.1 ± 0.3	83.1 ± 2.8	74.1 ± 3.5	73.3 ± 4.0
GM-3 (Ours)	98.2 ± 0.3	90.0 ± 1.0	94.2 ± 0.7	57.8 ± 5.5	44.8 ± 6.0	74.8 ± 3.6